

## Electrolytic characteristics of asymmetric alkyl carbonates solvents for lithium batteries

I. Geoffroy<sup>a</sup>, A. Chagnes<sup>a</sup>, B. Carré<sup>a</sup>, D. Lemordant<sup>a,\*</sup>, P. Biensan<sup>b</sup>, S. Herreyre<sup>b</sup>

<sup>a</sup>Laboratoire de Physicochimie des Interfaces et Milieux Réactionnels (EA2098), Faculté des Sciences et Techniques, Université de Tours, Parc de Grandmont, F 37200 Tours, France

<sup>b</sup>SAFT, Direction de la Recherche, 111 Boulevard A. Daney, 33074 Bordeaux, France

Received 20 February 2002; received in revised form 17 June 2002; accepted 1 July 2002

### Abstract

Asymmetric alkyl carbonate solvents (ACS) have been used as components of liquid electrolyte systems designed for Li-ion cells. Four ACS were selected: methyl-propyl carbonate (MPC), ethyl-propyl carbonate (EPC), methyl-isopropyl carbonate (MiPC) and ethyl-isopropyl carbonate (EiPC). The common features of all these ACS are a low melting point and a low viscosity, enhancing electrolytes conductivity toward low temperatures. The viscosity and the conductivity (salt: LiPF<sub>6</sub>, 1 M) of the ACS and their mixtures with ethylene carbonate (EC, 50% v/v), were studied as a function of the temperature (*T*). Arrhenius types plots of the logarithm of the conductivity versus 1/*T* reveals that ACS and ACS/EC mixtures are vitreous at low temperatures. The electrochemical and cycling behaviors of a graphite anode and a LiCoO<sub>2</sub> cathode have been evaluated using coin cells with a Li counter electrode. The charge and discharge capacities have been determined as a function of the cycle number. MiPC which builds an highly stable surface film on the graphite electrode, can be used as a single-solvent electrolyte with only a slight decrease in capacity of the LiCoO<sub>2</sub> cathode. All ACS/EC mixtures exhibit good filming properties at the negative electrode and no capacity loose at the positive electrode. The ability of some of the electrodes–electrolyte systems to undergo increased rates of discharge (*C*/5 to *C*/2) has been also evaluated.

© 2002 Elsevier Science B.V. All rights reserved.

**Keywords:** Organic electrolyte; Viscosity; Conductivity; Lithium battery; Asymmetric alkylcarbonate

### 1. Introduction

Since the introduction of Li-ion batteries in the 1990s, significant efforts have been made to improve the capacity and cycle life of anodic and cathodic materials [1]. One clue of these progresses is the choice of the electrolyte. Highly stable surface films are formed on the anode in the presence of some solvents like ethylene carbonate (EC) and alkyl carbonates [2,3]. The formation of a passive layer is required to allow reversible intercalation at the graphite anode [4]. At the same time, electrolytes used in high energy density Li batteries have to present a high conductivity, even at low temperature [5]. For this purpose, electrolytes based on solvents mixtures are usually chosen. Up to now, electrolytes are mostly constituted by a mixture of solvents with high permittivity (EC) and low viscosity (DMC, DEC) in order to promote simultaneously ionic dissociation and ion mobility [6]. Nevertheless, EC/DMC and EC/DEC electrolytes suffer

from their poor low temperature performance and exhibit low flash point (18 and 31 °C, respectively). In this paper, we introduce ACS as single solvent or cosolvent in the presence of the salt LiPF<sub>6</sub> as electrolytes for Li-ion cells.

In spite of their relatively low permittivity ( $\epsilon_r \approx 3-5$ ), asymmetric alkyl carbonate solvents (ACS) present promising properties such as low melting points, relatively high boiling points (>100 °C), low viscosities and large electrochemical windows [7]. In order to increase the permittivity of the electrolyte and hence to improve ion dissociation, EC has been used as cosolvent. The viscosity and the conductivity of LiPF<sub>6</sub> solutions in ACS and ACS/EC mixtures have been determined in order to optimize the composition of the electrolytes. The conductivity behavior at low temperature has also been considered since commercial cells require a low resistance especially at negative temperatures. The electrochemical performances of a graphitic negative electrode and a lithiated cobalt oxide cathode have been evaluated using a half cell design. It is essential to obtain good cycling properties, a long life and low fading.

\* Corresponding author. Tel.: +33-2-4736-6960; fax: +33-2-4736-6960.  
E-mail address: lemordant@univ-tours.fr (D. Lemordant).

## 2. Experimental

### 2.1. Preparation and purification of alkyl carbonate asymmetric

ACS were prepared in one step by a nucleophilic attack of an alcohol ROH on the RCOCl carbonyl group [8]. DMC and EC (purity >99%) were obtained from Fluka. LiPF<sub>6</sub> (purity 99%) was supplied by Merck. The water content of the electrolytic solutions was <50 ppm as indicated by Karl Fisher titration. Hereafter, LiPF<sub>6</sub> (1 M) ACS/EC will represent an electrolyte composed of the ACS and EC solvents mixed at the 1/1 volume ratio and the salt LiPF<sub>6</sub> at a concentration of 1 M (M = mol/l).

Viscosity was measured by the Ubbelohde capillary tube method using a Schott (AUS 310) viscometer. Densities were determined using a vibrating tube densimeter (Picker). Conductivity measurements were carried out using a conductivity cell with platinum electrodes and a CDM 230 conductivity meter (Meterlab).

The electrochemical experiments were run using a MacPile potentiostat for cyclic voltammetry and an Arbin electrochemical device equipment for cycling. Lithium metal electrodes were used as reference and/or auxiliary electrodes. The graphite and LiCoO<sub>2</sub> electrodes were provided by SAFT (Bordeaux). The graphite electrode is composed of a mixture of artificial graphites and has a theoretical capacity of 330 mAh/g.

## 3. Results and discussion

Four alkyl carbonates have been selected and synthesized for their physicochemical properties: methyl-propyl carbonate (MPC), methyl-isopropyl carbonate (MiPC), ethyl-propyl

carbonate (EPC) and ethyl-isopropyl carbonate (EiPC). Their physicochemical properties and those of the cosolvent EC are summarized in Table 1. In a comparison purpose, the characteristics of two symmetrical carbonates dimethyl carbonate (DMC) and diethyl carbonate (DEC) are also provided. They all exhibit a low melting point ( $\leq -50$  °C), a high boiling point ( $>100$  °C) and hence can be used as liquid solvents in a large range of temperatures. As their relative permittivities are of the same order of magnitude as DEC or DMC ( $\epsilon_r \approx 3-5$ ), the formation of numerous non-conducting ion pairs are expected. For this reason, a high permittivity cosolvent like EC has been added to the ACS in order to promote ion pairs dissociation and enhance the electrolyte conductivity.

### 3.1. Viscosity

Viscosity studies provide a useful insight on the mobility of ions in liquid or gel electrolytes. The viscosity at 25 °C of DMC, DEC, EC (at 40 °C), the pure ACS and their mixtures with EC are reported in Table 2. As expected from their higher molecular weight, the ACS are more viscous (values range from 0.80 to 1.1 mPa s) than their lighter homologues DMC, EMC and DEC. Nevertheless, their viscosities remain lower than those of the cyclic carbonates EC, PC or lactones (like  $\gamma$ -butyrolactone).

The geometry of molecules is an important factor to take into account when the viscosity of a solvent is considered. The presence of ramified alkyl chain in the molecular structure of dialkyl carbonates reduces the viscosity as seen for MiPC and EiPC when compared to their formula isomers MPC and EPC. As expected from the pure solvents values, ACS binary mixtures with EC are more viscous than the pure ACS but less viscous than EC.

In order to determine the influence of the temperature on the viscosities and, via the Stoke's law, on the ion mobilities,

Table 1  
Physical properties of solvents

Solvent	Formula	<i>M</i> (g/mol)	$\epsilon_r^a$	$\rho$ (g/cm <sup>3</sup> ) <sup>a</sup>	<i>t<sub>f</sub></i> (°C)	<i>t<sub>eb</sub></i> (°C)	$\mu$ (D)
DMC	C <sub>3</sub> H <sub>6</sub> O <sub>3</sub>	90	3.12	0.9764	4	90	2.95
DEC	C <sub>5</sub> H <sub>10</sub> O <sub>3</sub>	118	2.82	1.065	-44	127	2.62
MPC	C <sub>5</sub> H <sub>10</sub> O <sub>3</sub>	118	$\approx 3$	0.9795	-49	130	4.84
MiPC	C <sub>5</sub> H <sub>10</sub> O <sub>3</sub>	118	$\approx 3$	0.9698	-76	117	4.92
EPC	C <sub>6</sub> H <sub>12</sub> O <sub>3</sub>	132	$\approx 3$	0.9502	-81	148	5.25
EiPC	C <sub>6</sub> H <sub>12</sub> O <sub>3</sub>	132	$\approx 3$	0.9369	-132	135	-
EC	C <sub>3</sub> H <sub>4</sub> O <sub>3</sub>	88	89	1.3214	36.4	238	4.87

<sup>a</sup> At 25 °C, excepted for EC (40 °C).

Table 2  
Viscosity and activation energy at 298 K of the selected ACS and their binary mixtures (50% v/v) with EC

	Solvent/cosolvent											
	EC <sup>a</sup>	DMC	EMC	DEC	MiPC	EiPC	MPC	EPC	MiPC/EC	EiPC/EC	MPC/EC	EPC/EC
$\eta$ (mPa s)	1.9	0.59	0.65	0.75	0.86	0.98	1.08	1.13	2.00	2.25	2.08	2.29
$E_{a,\eta}$ (kJ/mol)	-	8.0	-	-	9.8	11.1	10.7	10.6	12.3	12.9	12.4	11.9

<sup>a</sup> At 40 °C.

viscosity measurements have been realized at different temperatures (25–55 °C). In this limited range of temperature, an Arrhenius comportment is expected and the relation proposed by Andrade [9] for non-associated liquids applies:

$$\eta = A_{\eta} \exp\left(\frac{E_{a,\eta}}{RT}\right) \quad (1)$$

In Eq. (1),  $E_{a,\eta}$  is the energy of activation for the viscosity and is obtained by plotting the logarithm of experimental viscosities ( $\ln \eta$ ) against  $1/T$ .  $E_{a,\eta}$  values for the ACS and their mixtures with EC are reported in Table 2. For the pure ACS, values range from 9.8 to 11.1 kJ/mol, significantly less their mixtures with EC (11.9–12.3 kJ/mol). The less viscous DMC has also a lower activation energy. As generally found in viscosity studies,  $E_{a,\eta}$  variations parallel  $\eta$  values when the liquid under consideration is changed.

$E_{a,\eta}$  is a thermodynamic function which reflects the sensitivity of the solvent viscosity to temperature variations. Addition of EC to ACS increases the activation energy and hence mixtures exhibit largest variations in viscosity with temperature than pure ACS. If the Stokes law applies, it is predicted that ion mobilities will be more sensitive to temperature variations in ACS/EC mixtures than in the pure ACS.

## 3.2. Conductivity

### 3.2.1. Conductivity at room temperature

The maximum of conductivity of  $\text{LiPF}_6$  solutions in ACS and ACS/EC mixtures is obtained for a molar concentration in salt of approximately 1 M. For this reason, only 1 M  $\text{LiPF}_6$  solutions are considered. The conductivities at 25 °C of the  $\text{LiPF}_6$  based electrolytes under consideration are reported in Table 3. ACS electrolytes are far less conducting than those obtained with EC or even DMC at the same concentration in salt. The addition of EC to ACS rises the conductivity of the electrolyte to values higher than 8 mS/cm, the conductivity of  $\text{LiPF}_6$  (1 M) in EC (at the exception

of EiPC/EC for which a lower value is found). The conductivity of the binary ACS/EC mixtures approaches 10 mS/cm at room temperature, but this is less the value obtained with the reference EC/DMC electrolyte (10.6 mS/cm). It is concluded that the main interest in the use of ACS as solvent for Li-ion batteries is not the conductivity.

### 3.2.2. Influence of the temperature

The conductivities of  $\text{LiPF}_6$  (1 M) in ACS and ACS/EC based electrolytes are plotted against the temperature in Figs. 1 and 2, respectively. The most striking feature is that electrolytes prepared from single solvents and mixtures exhibit a different behavior. When a single solvent is used, the variation in conductivity of the solutions increases steadily with the temperature but in the presence of ACS/EC mixtures, clear “S” shaped curves are obtained. The drop in conductivity of the ACS/EC electrolytes is sharp between 5 and  $-5$  °C and related to the apparition of a solid phase. EC is the component which has the highest fusion temperature and it is highly probable that this solid phase is mainly composed of EC molecules. Moreover, no crystallization occurs when PC is used instead of EC (MiPC/PC and EiPC/EC mixtures).

Beyond 5 °C, mixtures have higher conductivities than single solvents but when the temperature is lowered, crystallization occurs and, as a consequence, the conductivities of the solutions decrease drastically. Below  $-20$  °C, single solvent electrolytes become then far more conductive than mixtures which are in a solid or vitreous state.

Conductivities in ACS and ACS/EC mixtures do not follow an Arrhenius comportment but fits better the VTF equation [10–12]:

$$\kappa = AT^{1/2} \exp\left[\frac{-B}{T - T_0}\right] \quad (2)$$

where  $\kappa$  is the conductivity of the electrolyte and  $T_0$  the ideal glass transition temperature.  $AT^{1/2}$  is the pre-exponential factor and  $B$  is a parameter which has the dimension of an energy.  $A$  and  $B$  are considered as adjustable parameters. The ideal glass transition temperature  $T_0$  is the temperature at which the transport function ceases to exist or the solvent structural relaxation becomes zero and it has been found that in carbonate solvents containing Li salts,  $T_0$  was almost equal to the experimental  $T_g$  determined by DSC [13].

$T_0$  values, obtained from Eq. (2) by linear regression analysis of the conductivity–temperature data for single solvents and binary mixtures are reported in Table 4, together with some literature values. We can notice that, at the notable exception of the EPC +  $\text{LiPF}_6$ ,  $T_0$  values lie in a restricted range of temperature (143–173 K), independently of the nature of the Li salt used and the composition of the ACS/EC mixture. The addition of EC to the ACS +  $\text{LiPF}_6$  electrolyte rises  $T_0$ . This study supports the idea that in these media the conduction mechanism is of the solvent-assisted and controlled by the mobility of solvent molecules.

Table 3  
Conductivity ( $\kappa$  in mS/cm) at 25 °C of  $\text{LiPF}_6$  (1 M) in ACS and ACS/EC mixtures (50% v/v)

Solvent	$\kappa$ (mS/cm)
Single solvent	
EC	8.0
DMC	5.9
MPC	2.5
MiPC	1.8
EPC	1.8
EiPC	1.7
Binary mixture	
DMC/EC	10.6
MPC/EC	9.1
MiPC/EC	8.8
EPC/EC	8.2
EiPC/EC	7.7

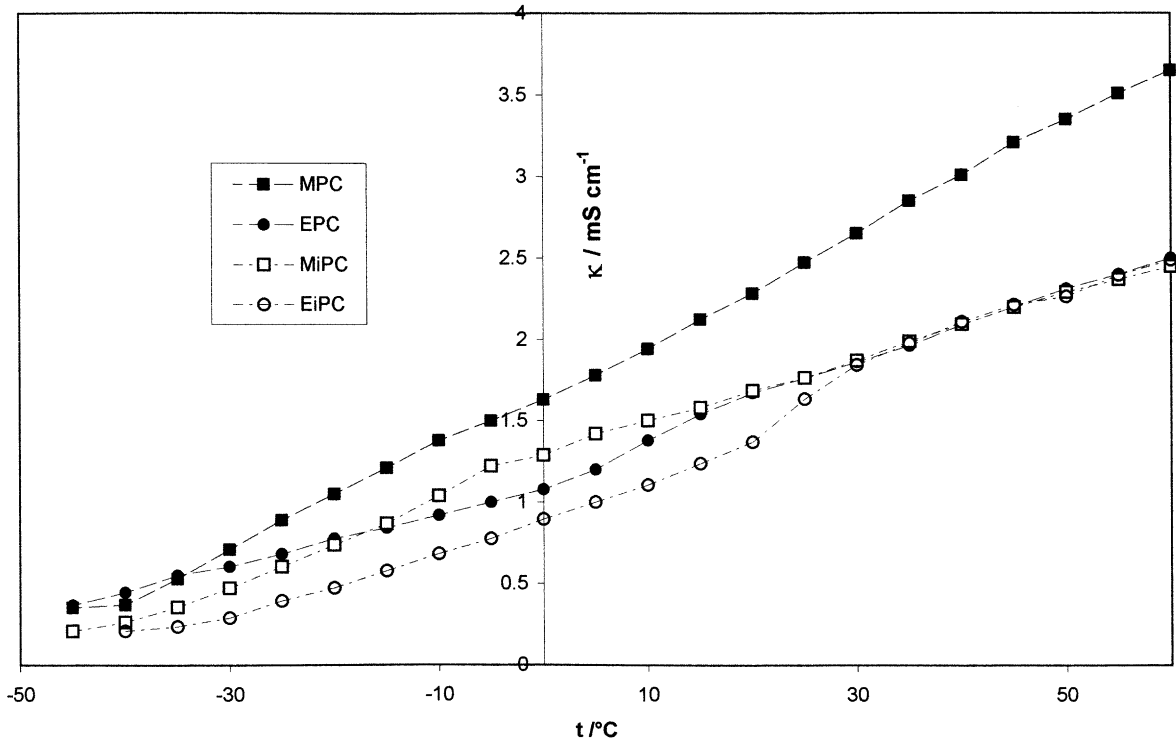


Fig. 1. Variation of conductivity of (1 M) LiPF<sub>6</sub> in ACS at different temperature.

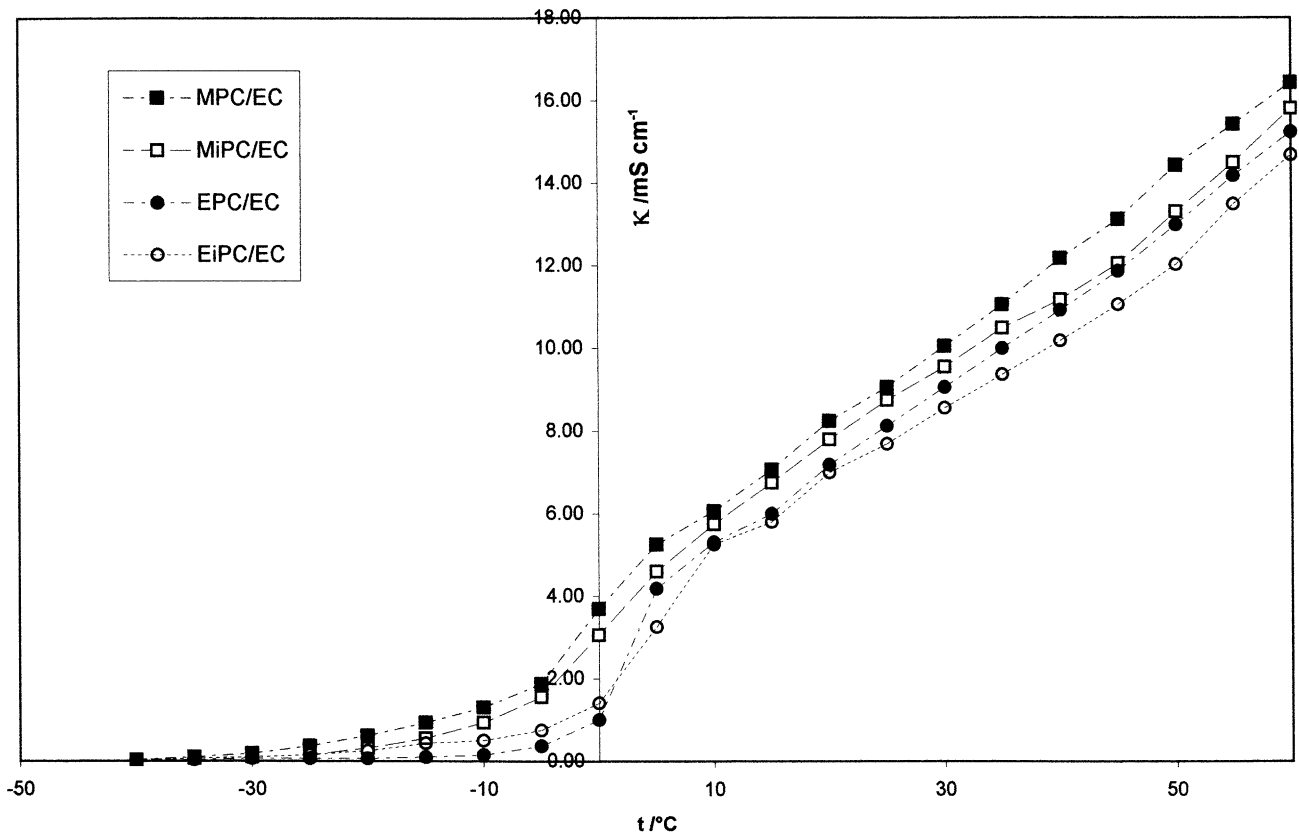


Fig. 2. Variation of conductivity of (1 M) LiPF<sub>6</sub> in ACS/EC mixtures (50% v/v) at different temperatures.

Table 4  
Ideal vitreous transition temperature  $T_0$  (in K) of ASC and ACS/EC (ratio in v/v) based electrolytes

Solvent	$T_0$ (K)
Single solvent	
MPC + LiPF <sub>6</sub> (1 M)	173
MiPC + LiPF <sub>6</sub> (1 M)	183
EPC + LiPF <sub>6</sub> (1 M)	73
EiPC + LiPF <sub>6</sub> (1 M)	143
Binary mixtures	
MPC/EC (1:1), LiPF <sub>6</sub> (1 M)	193
MPC/EC (2.2:1), LiAsF <sub>6</sub> (1 M)	151 <sup>a</sup>
MPC/EC (2.2:1), LiBetri (1 M)	165 <sup>a</sup>
MPC/EC (2.2:1), LiMethide (1 M)	164 <sup>a</sup>
MiPC/EC (1:1), LiPF <sub>6</sub> (1 M)	188
MiPC/EC (2.2:1), LiAsF <sub>6</sub> (1 M)	162 <sup>a</sup>
MiPC/EC (2.2:1), LiBetri (1 M)	164 <sup>a</sup>
MiPC/EC (2.2:1), LiMethide (1 M)	165 <sup>a</sup>
EPC/EC (1:1), LiPF <sub>6</sub> (1 M)	148
EiPC/EC (1:1), LiPF <sub>6</sub> (1 M)	173

Proportion of components in mixtures are in volume.

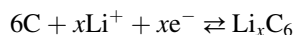
<sup>a</sup> From [13].

### 3.3. Electrochemical behavior

#### 3.3.1. Cyclic voltammetry

The electrochemical behavior of a composite graphite electrode was studied in the ACS based electrolytic solutions. The formation of the passive layer resulting from the reduc-

tion of solvent on the electrode surface has been studied by means of cyclic voltammetry. As an example, the voltammetric curve obtained in the EiPC/EC + LiPF<sub>6</sub> electrolyte is illustrated in Fig. 3. The first peak, near 0.8 V (versus Li<sup>+</sup>/Li), corresponds to the formation of the passive layer on the graphite electrode. Reduction potentials of approximately 0.7 V have been found for MPC, EPC, MiPC and the reference EC/DMC mixture. The formation of the SEI occurs at the same potential for all carbonates. The following reduction peaks are attributed to lithium intercalation into the graphite, according to the following reaction [14,15]:



The electrochemical behavior of a LiCO<sub>2</sub> electrode in the electrolyte EiPC/EC + LiPF<sub>6</sub> is reported in Fig. 4. Three successive oxidation peaks are observed on the voltammogram. The first peak is associated to the de-intercalation of the Li ions according to:



The two following peaks, between 4.2 and 4.8 V are attributed to phase transition occurring in the electrode material. Solvent oxidation on the LiCoO<sub>2</sub> electrode occurs at 5.1 V (EPC), 5.3 V (MiPC) and 5.5 V (MPC and EiPC). The ACS oxidation potentials are not very different than that of the reference EC/DMC mixture (5.5 V). These results show that these ACS have a quite wide electrochemical window.

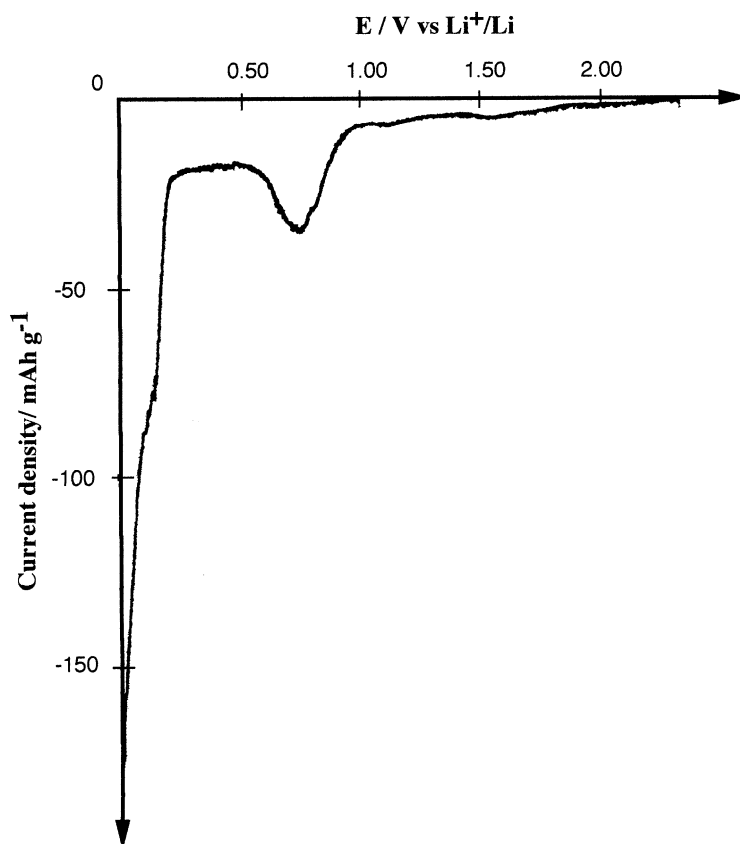


Fig. 3. Linear sweep voltammetry (50  $\mu$ V/s) of EiPC/EC + LiPF<sub>6</sub> (1 M) electrolyte at a graphite electrode.

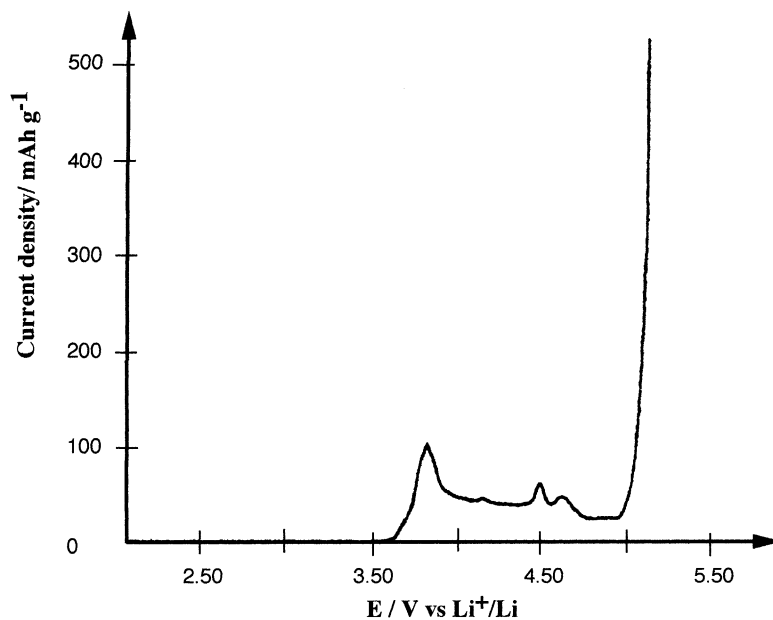


Fig. 4. Linear sweep voltammetry (10  $\mu\text{V/s}$ ) of EPC/EC +  $\text{LiPF}_6$  (1 M) at a  $\text{LiCoO}_2$  composite electrode.

### 3.3.2. Galvanostatic cycling

Two half cells, graphite/Li(metal) and  $\text{LiCoO}_2$ /Li(metal), have been used to determine the reversible/irreversible capacities, the coulombic efficiency (CE), the fading behavior of the graphite and  $\text{LiCoO}_2$  electrode and the capability of the graphite to undergo fast discharge rates. One single solvent (MiPC) and five mixtures (EC/DMC, MPC/EC, MiPC/EC, EPC/EC and EiPC/EC) have been selected for this study.

### 3.3.3. Graphite half cell

The cycling capacities have been determined by chronovoltammetry at constant rate of charge and discharge ( $C/20$ ). As an example, Fig. 5 presents the first cycle (potential versus capacity) of the graphite electrode in the EPC/

EC +  $\text{LiPF}_6$  electrolytic solution. The reversible capacity is 275 mAh/g while the irreversible capacity loss reached 64 mAh/g. In addition, no fading was noticed during the first 20 cycles at 60 °C.

Cycling results are summarized in Table 5. The reversible and irreversible charge capacities at the first cycle are noted  $C_{\text{rev}}$  and  $C_{\text{irr}}$ . For the subsequent cycles, the charge ( $C_{\text{ch}}$ , corresponding to Li intercalation), discharge capacities (Li de-intercalation  $C_{\text{dch}}$ ), and coulombic efficiencies (CE), are reported as a function of the cycle number. In agreement with previous results [8], the graphite electrode could not be cycled in EPC and EiPC solutions.

The reversible capacities loss obtained at the first cycle are lower than the theoretical capacity of the active material

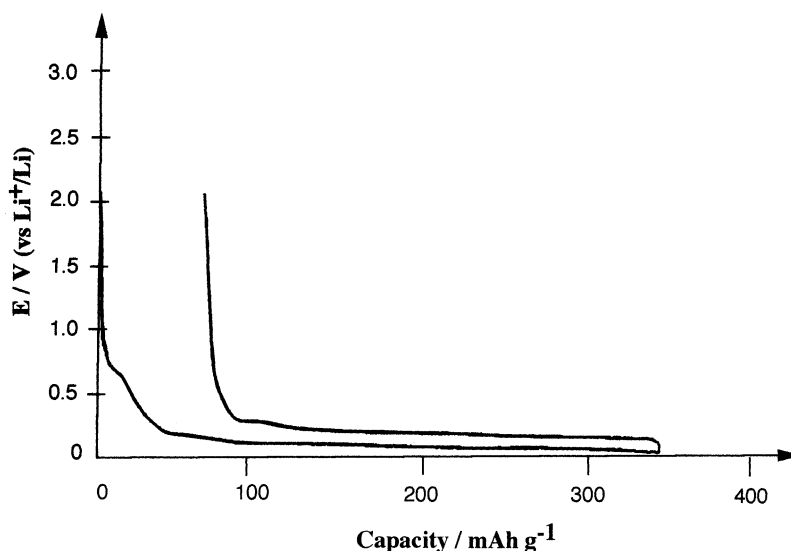


Fig. 5. Voltage capacity curve at a graphite electrode for the first intercalation–deintercalation cycle ( $C/20$  rate) in EPC/EC +  $\text{LiPF}_6$  (1 M).

Table 5

Charge ( $C_{\text{ch}}$ ) and discharge ( $C_{\text{dch}}$ ) capacities, and coulombic efficiencies (CE) as a function of the cycle number at the graphite composite electrode

	Solvent $x + \text{LiPF}_6$ (1 M)					
	$x = \text{EC/DMC}$	$x = \text{MiPC}$	$x = \text{MPC/EC}$	$x = \text{MiPC/EC}$	$x = \text{EPC/EC}$	$x = \text{EiPC/EC}$
First cycle						
$C_{\text{rev}}$	272	277	287.5	242	275.5	129
$r$ (%) <sup>a</sup>	100	102	106	89	101	47
$C_{\text{irr}}$	37	61	25	21	64	33
Second cycle						
$C_{\text{ch}}$	295	301.0	287			295.0
$C_{\text{dch}}$	295	299.5	284			294.8
CE (%) <sup>b</sup>	100	99.5	99			99.9
Fifth cycle						
$C_{\text{ch}}$		279.4		253	272.2	270.3 (224.1)
$C_{\text{dch}}$		279.4		236.9	288.6	270.3 (223.0)
CE (%)		100		93.6	106	100 (99.5)
Tenth cycle						
$C_{\text{ch}}$	264	278 (277.1)		241.3	292.4	269.2 (264.6)
$C_{\text{dch}}$	264	277.8 (275.4)		240.1	290.9	269.2 (263.8)
CE (%)	100	99.9 (99.4)		99.5	99.5	100 (99.7)
Fifteenth cycle						
$C_{\text{ch}}$		278.0			252.9	257.8
$C_{\text{dch}}$		277.8			247.8	257.8
CE (%)		99.9			98.0	100

For the first cycle, the reversible ( $C_{\text{rev}}$ ) and ( $C_{\text{irr}}$ ) irreversible capacities are indicated. All capacities (in mAh/g) are obtained at 25 °C,  $C/20$  charge and discharge and within 0.01–2.5 V limits.

<sup>a</sup>  $r = 10^2 [C_{\text{rev}}(\text{solvent } x)/C_{\text{rev}}(\text{EC/DMC})]$ .

<sup>b</sup>  $\text{CE} = 10^2 (C_{\text{dch}}/C_{\text{ch}})$ ; values in brackets correspond to duplicate experiments.

but close to that of the reference EC/DMC mixture for EC/DMC, MiPC, MPC/EC and EPC/EC. Lower values are found for MiPC/EC and EiPC/EC. In order to permit comparison with published data, the ratio ( $r$ , in %) of the discharge capacity in the considered electrolyte  $C_{\text{dch}}$  (solvent) to that in the reference EC/DMC mixture ( $C_{\text{dch}}$  (EC/DMC)) at the same cycle number, has been considered. First cycle  $r$  values for MiPC ( $r = 86\%$ ) or EPC/EC (89%), taken from Ein-Eli's results [8], are significantly lower than the present values (respectively, 102 and 101%), but the reverse is noted for the EiPC/EC mixture (89% against 47%).

The irreversible capacities fall in the range 21–64 mAh/g which can be considered as satisfactory. More significant, from a practical point of view, are the capacity fade and the gap between charge and discharge at each cycle (coulombic efficiency, CE). Coulombic efficiency values reported in Table 5 are close to 100% in most cases. The lowest value (CE = 93.6%) is found for MiPC/EC at the fifth cycle. This indicates that the capacity fade, over at least 15 cycles, is negligible. At the opposite to what has been previously claimed [8], no capacity gap between charge and discharge capacities is noted for MiPC. Surprisingly, the addition of EC to MiPC do not lead to better results in terms of capacities and coulombic efficiencies.

The fast discharge capability of the graphite half cell has been investigated using “power test”. This test consists into intercalating fast discharge rate ( $C/5$  and  $C/2$ ) between two

or three full cycles at  $C/15$ . As the charging rate of the graphite electrode is always low ( $C/15$ ), a complete lithiation of the electrode ( $x = 1$ ) is achieved. When the rate of discharge is increased to  $C/15$  or  $C/2$ , the ability of the cell to deliver an increased power during the discharge is evaluated. This power is largely dependent on the polarization resistance which itself comprises many components of ionic, electronic and diffusion character. Results concerning EC/DMC, MiPC, and EiPC/EC are reported in Table 6. The discharge capacities are high even at the fastest  $C/2$  rate of discharge. The coulombic efficiency is quite important and always higher than 94%: 94% in EiPC/EC and 96.4% in MiPC. This demonstrates the power capability of the graphite electrode when cycling in MiPC, as single solvent and EiPC/EC as mixed solvent.

### 3.4. Half cell with a $\text{LiCoO}_2$ electrode

Electrochemical studies of button cell composed of  $\text{LiCoO}_2$  as working electrode and lithium as counter electrode were performed in order to determine the cycling abilities of the cathode in these electrolytes. The cell were cycled at room temperature, using  $C/30$  rate of charge and discharge in the potentials limits 3.0–4.2 V. In Fig. 6 is reported the first cycle potential–capacity curve of the  $\text{LiCoO}_2$  in EPC/EC electrolyte. The reversible capacity is equal to 146 mAh/g and the irreversible capacity is 3 mAh/g.



Table 6  
Power test on the graphite electrode

		Rate of discharge								
		C/15	C/15	C/5	C/15	C/15	C/15	C/2	C/15	C/15
MiPC + LiPF <sub>6</sub> (1 M)	C <sub>dch</sub>	297.4	296.4	290.7	295.7	296.0	296.9	286.7	295.8	296.2
	CE (%)			97.7		99.5		96.4		99.6
EiPC/EC + LiPF <sub>6</sub> (1 M)	C <sub>dch</sub>	300.0	298.5	282.3	296.8	298.1	297.9	282.0	295.3	296.8
	CE (%)			94		99.4		94		99
EC/DMC + LiPF <sub>6</sub> (1 M)	C <sub>dch</sub>	293.1	302.8	286.0	288.6	288.3	288.2	277.9	289.5	290.9
	CE (%)			97.6		98.4		94.8		99.2

Discharge capacities (C<sub>dch</sub>) are in mAh/g. The coulombic efficiency (CE) is the ratio 10<sup>2</sup>(C<sub>dch</sub>/C<sub>ch</sub>).

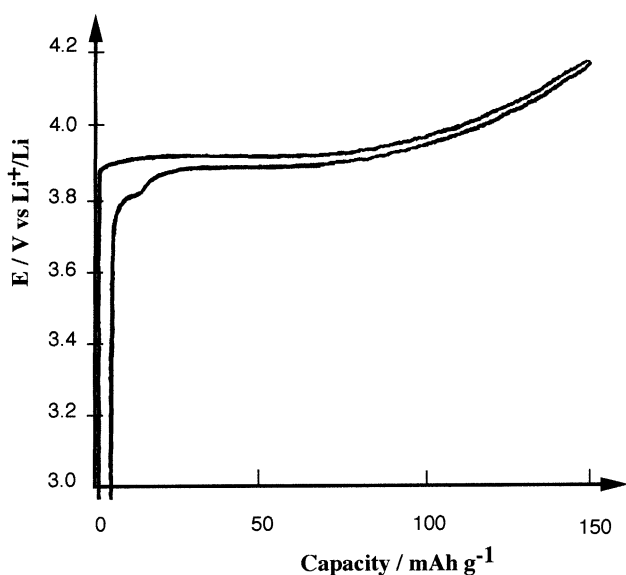


Fig. 6. Voltage capacity curve at a LiCoO<sub>2</sub> composite electrode for the first deintercalation–intercalation cycle (C/30 rate) in EPC/EC + LiPF<sub>6</sub> (1 M).

Table 7

Cycling behavior of a LiCoO<sub>2</sub> electrode in MiPC and ACS/EC mixture at 25 °C and C/30 galvanostatic charge and discharge within the 3.0–4.2 V limits

	Solvents				
	MiPC	MPC/EC	MiPC/EC	EPC/EC	EiPC/EC
First cycle					
C <sub>rev</sub>	116.7 <sup>a</sup>	145.5	143.4	146	133
C <sub>irr</sub>		5.6	5.6	3	8
Fifth cycle					
C <sub>dch</sub>	111			145	139

Capacities are in mAh/g.

<sup>a</sup> Second cycle.

Cycling results for the cathode are gathered in Table 7. After five cycles, the reversible capacity remains equal to 145 mAh/g. No capacity fading is noted, at least over the five first cycles and similar results are obtained with MPC/EC and EiPC/EC electrolyte. In the case of MiPC, the electrode is cycling but with a reduced capacity (–23%).

#### 4. Conclusion

In spite of their low permittivity, ACS are interesting solvents as they have a low viscosity and remain fluid at very low temperatures. Mixed with EC, solutions are more viscous but also more conducting owing to the dissociation power of EC toward the ion pairs. Conductivity studies show that ACS + LiPF<sub>6</sub> solutions exhibit, at low temperatures, a vitreous transition from which the ideal temperature of glass formation can be inferred.

A good quality passive layer with very few exfoliation is formed on the graphite electrode in MiPC and the ACS/EC mixtures. For this reason, the charged capacity is recovered to close to 100% at each cycle. As in the EC/DMC reference electrolyte, the charge–discharge capacities are less by 10–15% than the theoretical capacity of the active material. The capacity fade does not exceed 10–15% over 15 cycles. The ability of the graphite half cell to undergo rapid rate of discharge (C/5 to C/2) is good as the capacity loose is <3%. The cathodic LiCoO<sub>2</sub> active material exhibit good cycling results with ACS/EC mixtures, but with a reduced capacity when MiPC is used as a single solvent.

#### References

- [1] H. Tamura, J. Power Sources 81/82 (1999) 156.
- [2] E. Peled, J. Electrochem. Soc. 126 (1979) 2047.
- [3] E. Peled, in: J.P. Gabano (Ed.), Lithium Batteries, Academic Press, London, 1943, p. 43.
- [4] C.A. Vincent, Solid State Ionics 134 (2000) 159.
- [5] E.J. Plichta, W.K. Behl, J. Power Sources 88 (2000) 192.
- [6] I. Geoffroy, P. Willmann, K. Mesfar, B. Carre, D. Lemordant, Electrochim. Acta 45 (2000) 2019.
- [7] J.S. Foos, T.S. Solki, X. Beebe, J. Electrochem. Soc. 27 (1998) 2.
- [8] Y. Ein-Eli, S.F. Mc Devitt, R. Laura, J. Electrochem. Soc. 145 (1998) 1.
- [9] E.N. Andrade, Nature 125 (1930) 309.
- [10] H. Vogel, Phys. Z. 22 (1921) 645.
- [11] G. Tammann, W. Hesse, Z. Anorg. Allg. Chem. 156 (1926) 245.
- [12] G.S. Fulcher, J. Am. Ceram. Soc. 8 (1925) 339.
- [13] G.Y. Gu, R. Laura, K.M. Abraham, Electrochem. Solid State Lett. 2 (1999) 486–489.
- [14] A. Herold, Bull. Soc. Chim. 187 (1995) 999.
- [15] D. Guérard, A. Herold, Carbon 13 (1975) 337.